Proceedings of the 29th Polish-Slovak Scientific Conference on Machine Modelling and Simulations 2024, Poland

Numerical Modeling of Basic Physical Phenomena of the Cast Slab Solidification Process at the Initial Stage of the Continuous Casting Process

L. Sowa*

Czestochowa University of Technology, Faculty of Mechanical Engineering, Dąbrowskiego 73, 42-201 Częstochowa, Poland

Doi: 10.12693/APhysPolA.145.756 *e-mail: leszek.sowa@pcz.pl

Understanding the complex physical phenomena involved in the continuous casting process simulation requires continuous and complementary research to improve mathematical modeling. The paper presents a mathematical model and numerical simulations of the molten steel flow by the submerged entry nozzle and the filling process of the continuous casting mold cavity. In the mathematical model, the temperature fields were obtained by solving the energy equation, while the velocity fields were calculated by solving the momentum equations and the continuity equation. These equations contain the turbulent viscosity, which is found by solving two additional transport equations for the turbulent kinetic energy and its rate of dissipation. In the numerical simulations, coupling of the thermal and fluid flow phenomena by changing the thermophysical parameters of alloy depending on the temperature has been taken into consideration. The finite element method was used to solve this problem. Numerical simulations of filling the continuous casting mold cavity were performed for two variants of liquid metal pouring. The effect of the cases of pouring the continuous casting mold on the velocity fields and the solid phase growth kinetics in the process of filling the continuous casting mold was evaluated. It turns out that the appropriate selection of the submerged entry nozzle is very important for the failure-free operation of the continuous casting machine and obtaining a high-quality slab, which was the purpose of this work.

topics: numerical simulations, solidification, continuous steel casting

1. Introduction

The continuous steel casting (CSC) process has been intensively developed in recent years because it is characterized by better performance and thermal efficiency than casting to ingot molds [1, 2]. Due to the difficulties in empirical research of this process, numerical simulations are becoming an important tool for analyzing the thermal-flow phenomena of the CSC process. Therefore, there is a need to formulate coupled mathematical models that take into account these phenomena [1–7], which was done in this work. It is noted that for the movements of liquid metal in a continuous casting mold (CCM), the appropriate selection of the type of submerged entry nozzle (SEN) is of great importance. This enables control of the flow of liquid steel, which allows for the separation of non-metallic inclusions and their transport to the slag layer [2–7]. The aim of this work is therefore to assess the impact of pouring methods (two types of SEN) on the movements of liquid metal and the growth kinetics of the solid phase in a rectangular cast slab in the initial phase of the CSC process. These activities are aimed at improving the strength properties of the obtained steel.

2. Mathematical model

The mathematical description of molten metal flow within the continuous casting mold cavity during the filling has been proposed. It has been assumed that the solidification front is mushy [1–7]. The mathematical model is based on the solution of the following system of differential equations (the energy equation, the momentum equations, and the continuity equation) [3–7]

$$\rho C_{ef}\left(\frac{\partial T}{\partial t}+v_j\frac{\partial T}{\partial x_j}\right)=\frac{\partial}{\partial x_j}\left(\lambda\frac{\partial T}{\partial x_j}+\frac{c\mu_t}{\sigma_t}\frac{\partial T}{\partial x_j}\right), \tag{1}$$

$$\rho\left(\frac{\partial v_i}{\partial t}+v_j\frac{\partial v_i}{\partial x_j}\right)=-\frac{\partial p}{\partial x_i}+\rho g_i + \frac{\partial}{\partial x_j}\left((\mu+\mu_t)\left(\frac{\partial v_i}{\partial x_j}+\frac{\partial v_j}{\partial x_i}\right)-\frac{2}{3}\rho k\delta_{ij}\right), \tag{2}$$

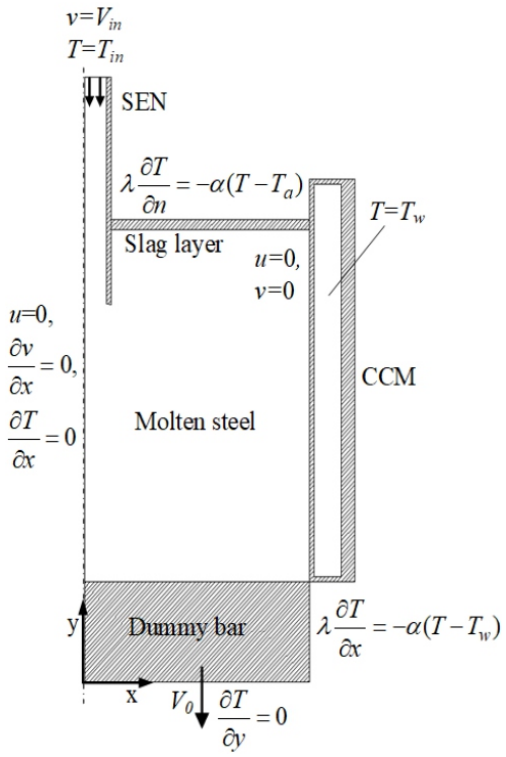

Fig. 1. Schematic illustration of the continuous casting mold and boundary conditions.

$$\nabla \cdot \boldsymbol{v} = 0. \tag{3}$$

The turbulence dynamical viscosity coefficient (μ_t) occurring in (1) and (2) is defined as follows

$$\mu_t = c_\mu \rho \frac{k^2}{\varepsilon}. \tag{4}$$

In the above formula, k and ε are obtained from the following equations (the equation for turbulence kinetic energy and equation for dissipation rate of turbulence kinetic energy) [3–6]

$$\rho\left(\frac{\partial k}{\partial t} + v_j \frac{\partial k}{\partial x_j}\right) = \frac{\partial}{\partial x_j}\left((\mu + \frac{\mu_t}{\sigma_k})\frac{\partial k}{\partial x_j}\right) + \mu_t \frac{\partial v_i}{\partial x_j}\left(\frac{\partial v_i}{\partial x_j} + \frac{\partial v_j}{\partial x_i}\right) - \frac{\mu_t}{\rho \sigma_\rho}\frac{\partial \rho}{\partial x_i} g_i - \rho\varepsilon, \tag{5}$$

$$\rho\left(\frac{\partial \varepsilon}{\partial t} + v_j \frac{\partial \varepsilon}{\partial x_j}\right) = \frac{\partial}{\partial x_j}\left((\mu + \frac{\mu_t}{\sigma_\varepsilon})\frac{\partial \varepsilon}{\partial x_j}\right) - \frac{c_2 \rho \varepsilon^2}{k} + \frac{c_1 \varepsilon \mu_t}{k}\frac{\partial v_i}{\partial x_j}\left(\frac{\partial v_i}{\partial x_j} + \frac{\partial v_j}{\partial x_i}\right) - \frac{c_1(1-c_3)\varepsilon}{k}\frac{\mu_t}{\rho\sigma_\rho}\frac{\partial \rho}{\partial x_i} g_i, \tag{6}$$

where T is the temperature [K], λ is the thermal conductivity coefficient [W/(m K)], v_j is the velocity vector of liquid metal flow [m/s], p is the pressure [N/m^2], $\rho = \rho(T)$ is the density [kg/m^3], $C_{ef}(T) = c_{LS} + L/(T_L - T_S)$ is the effective specific heat of a mushy zone [J/(kg K)] [2, 6], c_{LS} is the specific heat of a mushy zone [J/(kg K)], L is the latent heat of solidification [J/kg], $\mu(T)$ is the dynamical viscosity coefficient [Ns/m^2], c is the specific heat [J/(kg K)], T_L and T_S are respective liquidus and solidus temperatures of the analyzed alloy [K], g_i is the vector of the gravity acceleration [m/s^2], μ_t is the turbulence dynamical viscosity coefficient [N s/m^2], k is the turbulence kinetic energy [m^2/s^2], ε is the dissipation rate of turbulence kinetic energy [m^2/s^3], t is time [s], and x_j is the coordinates of vector of a node's position [m]. As for $\sigma_t = 0.9$, $\sigma_\varepsilon = 1.3$, $\sigma_p = 0.9$, $c_1 = 1.44$, $c_2 = 1.92$, $c_3 = 0.8$, $c_\mu = 0.09$, $\sigma_k = 1$, they are all empirical constants [3–6].

The system of equations (1)–(6) is completed by the initial conditions and appropriate boundary conditions, which are shown in Fig. 1 [2, 4–6]. For (4)–(6), the zero value k and ε on the walls of continuous casting mold was assumed [5].

The above problem was solved by using the finite element method in the weighted residuals formulation [2, 6].

3. Examples of numerical calculations

The calculations were performed for the continuous casting mold with a rectangular cross-section cavity of 0.28×1 m and a length of 0.85 m.

The superheated steel with temperature $T_{in} = 1850$ K was poured with velocity $V_{in} = 0.35$ m/s into the considered region with the initial temperature $T_M = 450$ K. The thermophysical properties of cast steel were taken from works [3, 5]. The characteristic temperatures of liquid steel were $T_L = 1810$ K and $T_S = 1760$ K, whereas the ambient and cooling water temperatures amounted

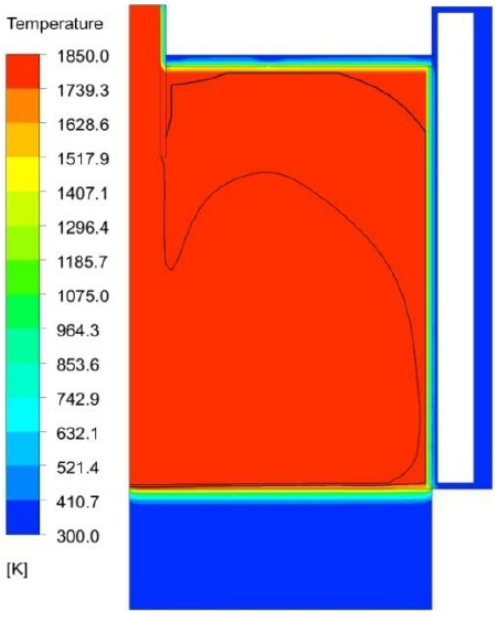

Fig. 2. Temperature field after time $t = 21$ s, I variant.

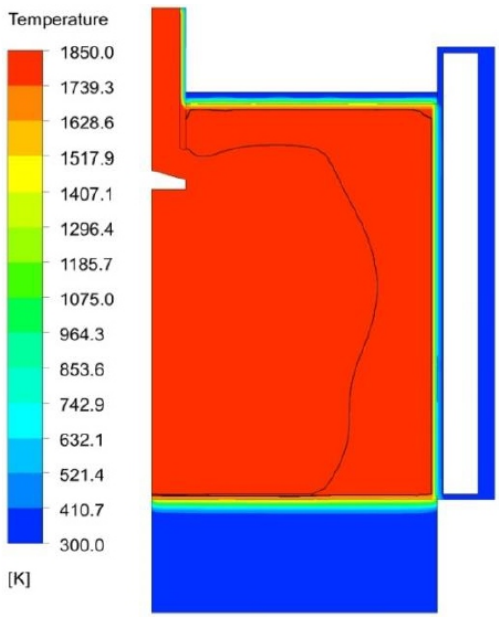

Fig. 3. Temperature field after time $t = 21$ s, II variant.

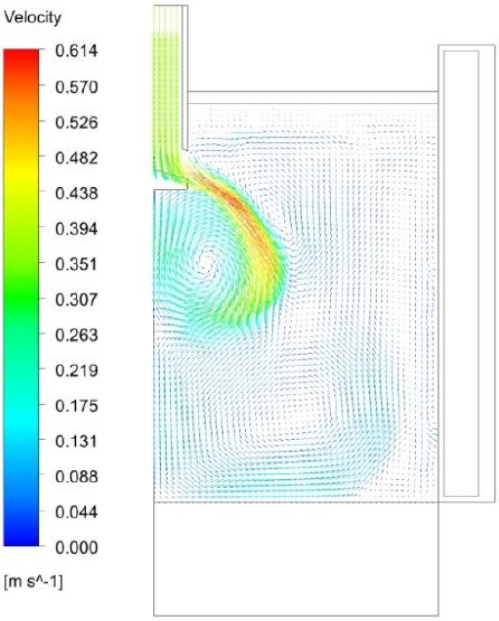

Fig. 4. Velocity vectors after time $t = 21$ s, II variant.

to $T_a = 300$ K and $T_w = 283$ K, respectively. The heat-transfer coefficient (α) between the continuous casting mold and ambient was equal $\alpha_m = 60$ W/(m^2 K) and between the slag and ambient $\alpha_s = 2$ W/(m^2 K) [1, 6]. The thermal and fluid flow phenomena occurring in the considered system were analyzed. The selected results of numerical simulations are shown in Figs. 2–4. The filling process of the continuous casting mold cavity was performed for two cases of liquid metal pouring: vertical (I variant) (Fig. 2) and horizontal (II variant) (Figs. 3, 4). The liquidus and solidus lines are visible on the temperature field presented in Figs. 2, 3. They indicate the current position of the two-phase zone, while the solidus line indicates the instantaneous thickness of the solid phase. In the area with a temperature higher than the liquidus line, there are intense movements of the liquid phase of the poured steel, which can be seen in the distribution of velocity vectors (Fig. 4).

4. Conclusions

The article mainly focused on the analysis of thermal and flow phenomena occurring in the continuous casting mold in the initial phase of the CSC process. The influence of a continuous casting mold pouring case on the velocity fields of the liquid phase and the kinetics of solid phase growth in the cast slab was assessed. It was observed that in the case of vertical and horizontal pouring, there are no significant differences in the thickness and shape of the solid phase formed on the walls of the continuous casting mold. This conclusion applies only to the filling period of the continuous casting mold (time 21 s, Figs. 2, 3). However, the pouring method seems to be important in the case of inclusion removal operations, which require the appropriate direction of the movement of liquid metal towards the slag layer. Numerical studies of the velocity distribution in a continuous casting mold have shown that the flow field generated by horizontal discharge nozzles is more favorable for inclusion removal. Changing the arrangement of non-metallic inclusions in the continuous casting mold has a significant impact on the surface state and mechanical properties of the resulting cast slab, which is important for foundry practice.

References

[1] S. Mosayebidorcheh, M. Gorji-Bandpy, *Appl. Therm. Eng.* **118**, 724 (2017).

[2] L. Sowa, *Arch. Foundry Eng.* **11**, 199 (2011).

[3] S. Lei, J. Zhang, X. Zhao, K. He, *ISIJ Int* **54**, 94 (2014).

[4] Y. Hashimoto, A. Matsui, T. Hayase, M. Kano, *Metall. Mater. Trans. B* **51**, 581 (2020).

[5] S. Yu, M. Long, M. Zhang, D. Chen, P. Xu, H. Duan, J. Yang, *J. Manuf. Process.* **68**, 1784 (2021).

[6] L. Sowa, T. Skrzypczak, P. Kwiatoń, *Arch. Foundry Eng.* **18**, 115 (2018).

[7] Z. Liu, B. Li, L. Zhang, G. Xu, *ISIJ Int.* **54**, 2324 (2014).